REGULAR PAPER

Effect of Groove Surface on Friction Noise and Its Mechanism

Jae-Hyeon Nam[1], Hyun-Cheol Do[1], and Jae-Young Kang[1,#]

1 School of Mechanical Engineering, College of Engineering, Kongju National University, 1223-24, Cheonan-daero, Seobuk-gu, Cheonan-si, Chungcheongnam-do, 31810, South Korea
Corresponding Author / E-mail: jkang@kongju.ac.kr, TEL: +82-41-521-9263, FAX: +82-41-554-6516

In this study, friction noise according to whether grooves exist was measured using a reciprocating sliding device, and the relationship between the groove and friction noise mechanism was investigated. Experimental results revealed that both non-groove textured and groove textured surfaces produced friction noise at approximately 5 kHz. However, the friction noise onset time was relatively faster and the sound pressure level was higher for the non groove textured surface. The tribo-surfaces of the plate and ball which change in time for the non-groove textured and groove textured surfaces were observed using a microscope. For the non-groove textured surface, adhesive wear was commonly observed on the tribo-surface, and for the groove textured surface, wear particles accumulated within the groove due to the movement of the ball, and adhesive wear appeared more slowly. As a result, the friction coefficient was relatively larger for the non-groove textured surface, facilitating the mode coupling instability. Using the pin-on-disk system, the propensity for the negative friction-velocity slope was also measured with regard to the non-groove textured surface.

1. Introduction

When two objects are in contact, friction occurs on the contact area due to the relative contact motion and wear occurs on the tribo-surface. Wear is the phenomenon where the contact surface is altered physically and chemically. This causes adhesive wear due to attractive and shearing forces on the friction contact area. Scuffing (blackening from friction heat) and scratching phenomena occur on the contact surface during the continuous friction behavior between the metallic materials. Such worn surfaces create debris from wear, influencing noise and vibration from the friction motion. Research on friction noise according to surface topography caused by dry friction has been widely carried out using friction experiments. Chen et al.[1,2] used a reciprocating system to investigate the relationships between the tribo-surface and friction coefficient as well as sliding speed and friction noise. Jibki et al.[3] also used a reciprocating system to examine the correlation between amount of wear and the friction coefficient on friction noise for the tribo-surface.

Unlike the non-groove textured surface, the groove textured surface is known to influence the reduction of the friction coefficient. Research on the friction behavior of the contact surface for the groove textured surface have been actively pursued. Yuan et al.[4] concluded that a perpendicular contact angle between the micro-groove textured surface and smooth surface is more effective in reducing the friction coefficient compared to when the contact angle is horizontal. Mo et al.[5] showed experimentally through a parametric study of the width and pitch parameters of the ball-on-flat (groove textured surface) that the friction coefficient was effectively reduced along with friction noise when the width-pitch ratio of the groove textured surface was 1/2. Saeidi et al.[6] studied the effect of surface texturing on friction behavior in starved lubrication conditions and showed that the geometrical texture parameters affect tribological performance and the lifetime of the tribo-system. Zhang et al.[7] developed an analytical model to understand the tribology behavior of surface texturing in mixed lubrication. Wang et al.[8,9] performed a reciprocating friction test for the ball-on-flat (groove-textured surface) and determined that a groove textured surface of specific conditions reduced the friction noise. Additionally, complex eigenvalue and dynamic transient analyses were conducted using a FE model to predict the friction noise. He et al.[10] showed experimentally that a micro-scale groove textured surface reduces the friction coefficient. Wang et al.[11] studied the effect of line contact on the friction coefficient depending on the radius of the cylinder and dimple size for the friction motion of line contact between a cylinder and dimple textured surface. Studies regarding the effect of surface topography were conducted on

Springer
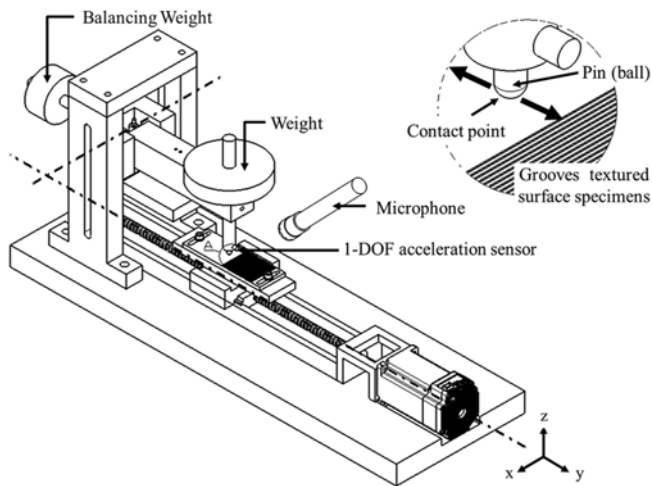
Fig. 1 Schematic diagram of the reciprocating system

the relationship among the contact surface topography, a friction coefficient and friction noise.[12,13]

However, studies which approached the mechanisms of friction noise for the groove-textured surface are rare. The major mechanisms for friction noise include mode coupling and instability caused by a negative friction-velocity slope of the friction curve.[14-17] Thus, in this paper, the friction noise for non-groove textured and groove textured surfaces were measured under the condition of ball-on-flat (grooved textured surface) using a reciprocating system and pin-on-disk system. Also, the mechanisms behind the noise were analyzed, and the tribo-surface topography was observed using a microscope to investigate the wear behavior associated with friction noise.

2. Experiment and Analysis

2.1 Experimental procedure of the friction noise

Fig. 1 shows the schematic diagram of the reciprocating system. The plate undergoes reciprocating motion by the rotation of the screw connected to the motor and friction occurs between the plate and ball due to the loading on the weight. During the reciprocating motion of the plate, the generated friction noise was measured using an accelerometer and microphone attached to the beam, and the friction coefficient can be measured using the force sensor. The friction noise experiment was carried out for 486 sec (30 cycles) with a load of 9.8 N and sliding speed of approximately 0.01 m/s.

Fig. 2 shows the plate and test mode used in the friction noise experiment. As can be observed in Fig. 2(a), the total reciprocating motion distance of the plate was 90 mm where 45 mm was the non-groove surface plate while the remaining 45 mm was the groove surface. Fig. 2(b) shows the groove depth of 0.15 mm and distance of 1 mm between each groove. Also, the diameter of one groove was 0.3 mm. Fig. 2(c) shows the friction noise test mode. The plate speed was approximately 0.01m/s and the reciprocating motion was carried out over a friction distance of 90 mm.

The plate material was steel (SS400) and the ball material was aluminum (A 6061 T6). Table 1 shows the material properties of each
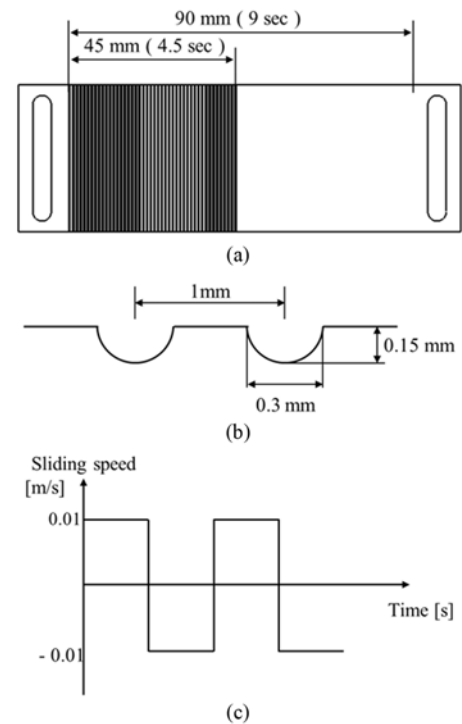
Fig. 2 Reciprocating test specimen and test mode; (a) reciprocating test specimen (b) dimension of groove (c) speed profile of friction noise test

Table 1 Material of the reciprocation system

Classification	Plate	Pin
Picture		
Material	Steel (SS400)	Al(A 6061 T6)
Density [kg/m^3]	7850	2700
Young's modulus [GPa]	205	68.9
Poisson ratio	0.3	0.33
Roughness (Ra) [μm]	1.0	0.8

specimen. The roughness of the pin surface was 0.8 μm and the test was conducted under dry friction conditions. Also the friction surfaces were cleaned by acetone to remove any contaminants before the every test.

2.2 Results with the experimental of friction noise

Fig. 3 shows the background noise generated by the operation of motor. Fig. 4 illustrates the frequency spectrum by taking the fast Fourier Transform (FFT) on the sound pressure for the total duration where friction noise occurs at about 5 kHz and this mode is defined as 'A'. From Figs. 3 and 4, the peak of the friction noise can be clearly found. The spectrograms were also used to analyze the friction noise pattern with time as shown in Fig. 5. The results correspond to the friction experiment carried out over 30 reciprocation cycles. Here, 'A' clearly distinguishes between the interval where friction noise occurs
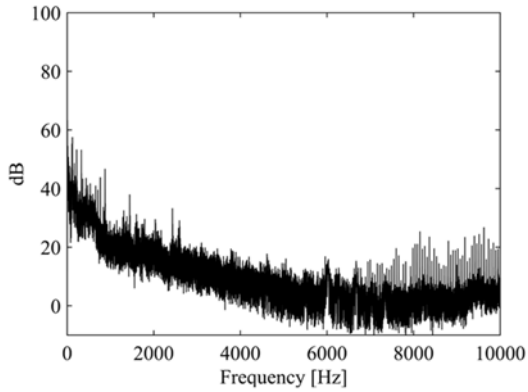
Fig. 3 Background noise of the reciprocating system
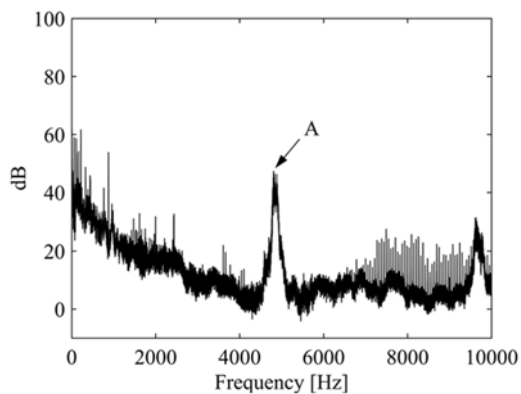
Fig. 4 PSD of the sound pressure

and the interval with no friction noise. Zone I is the interval of 1 cycle from 0 to 16 sec as shown in Fig. 5(b), and Zone II is the interval of 1 cycle from 400 to 416 sec as shown in Fig. 5(c). In Zone I, which is the initial state of friction, no friction noise is generated for both the non-groove surface of the plate. Friction noise was clearly generated starting at approximately 400 sec, but only in the +y direction, in the non-groove surface interval of Zone II where friction continued for a long time. Frequency B near 10 kHz is the second harmonic frequency of A.

In order to investigate the relationship between the friction coefficient and friction noise, additional reciprocating friction experiments were conducted by separating the non-groove and groove surfaces. Fig. 6 shows the friction coefficient variation with time for the non-groove and groove surfaces along with the vibration data from the accelerometer attached to the beam. The experiments were carried out for 700 sec with friction distances of 45 mm for each surface and speed of approximately 0.01 m/s.

As observable in Fig. 6(a), the friction coefficient for the non-groove surface increased for the +y direction as friction continued. On the other hand, as shown in Fig. 6(b), the friction coefficient for the groove surface was relatively smaller than that for the non-groove textured surface. Figs. 6(c) and 6(d) show the acceleration in time for the non-groove surface and groove surface, respectively. As can be observed in Figs. 6(c)-6(d), the vibration level of the groove surface was relatively low compared to the non-groove surface.
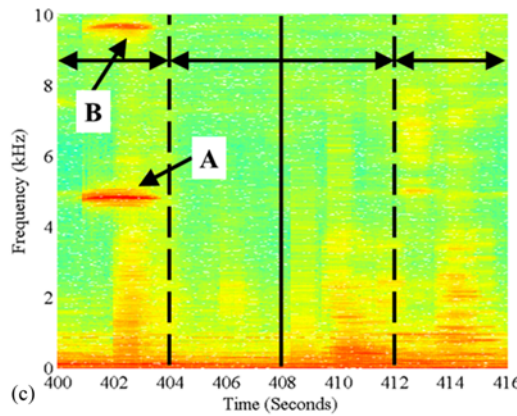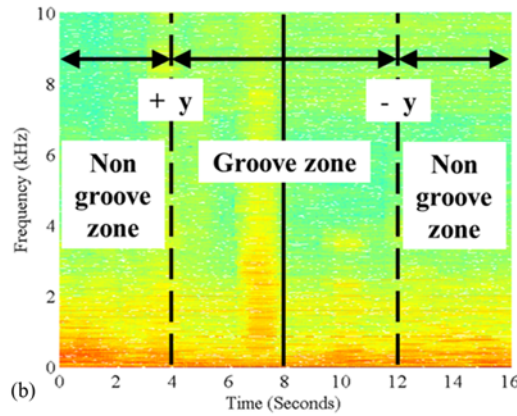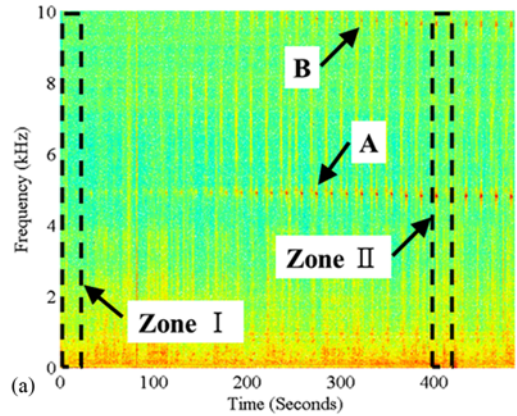
Fig. 5 Spectrogram: (a) sound pressure signal (b) spectrogram in the Zone I (c) spectrogram in the Zone II

Fig. 7 shows the RMS values of the vibration level magnitude was slightly higher for the groove-surface due to the vibration caused by the grooves up to 260 sec. It is noted, after 260 sec where friction noise occurred on the non-groove surface, the vibration level of the non-groove surface was drastically increased whereas the vibration level of the groove surface remains low. Also, as shown in Fig. 8, the RMS value of friction coefficient in Eq. (1) for the groove surface remains lower than the non-groove surface. The RMS of friction coefficient of the non-groove surface increases with time, implying that the increase of friction coefficient causes friction noise.

$$RMS(\mu) = \int_{t}^{t+20sec} \sqrt{\mu(t)^2} dt \qquad (1)$$
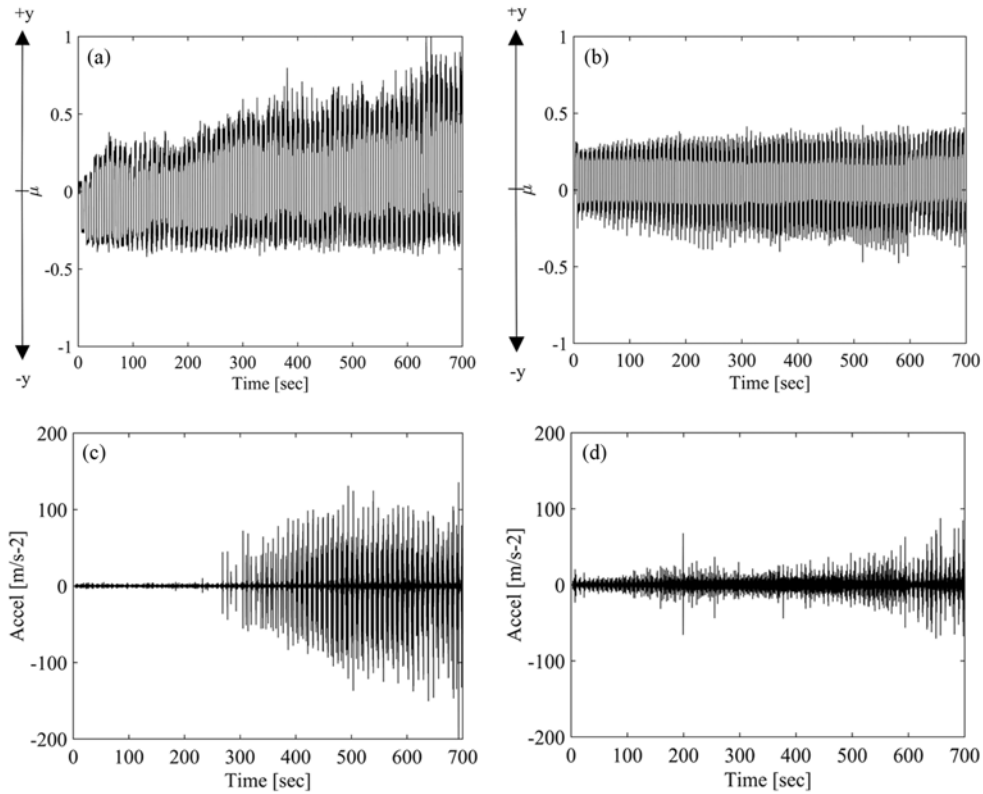
Fig. 6 Friction coefficient and vibrations: (a) friction coefficient of the non-groove surface (b) friction coefficient of the groove surface (c) accelerations of the non-groove surface (d) acceleration of the groove surface
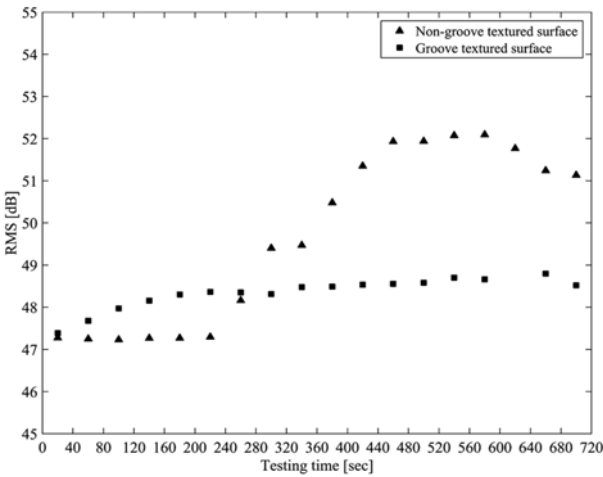
Fig. 7 RMS of acceleration level in time
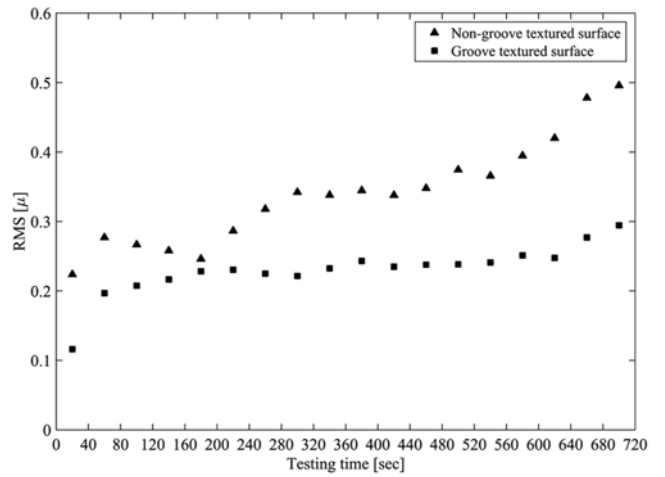
Fig. 8 RMS of friction coefficient in time

2.3 Experimental procedure of friction-velocity curve

Figs. 9(a) and (b) show the schematic diagram of the pin-on-disk device used to measure the friction curve with respect to the sliding speed for the non-groove and groove surfaces. The normal force applied in the pin-on-disk test was equivalent with the force used in the reciprocating experiment which was 9.8 N. Fig. 10 shows the test mode used to measure the friction curve and the dimensions of the grooves.

As show in Fig. 10(a), grooves were made on the disk and the fiction distance varied according to the contact position of the ball. Figs. 10(a) and (b) show the ball position corresponding to the disk

friction distance between the grooves of approximately 1 mm which is almost the same as the friction noise experiment condition using the reciprocating system. For the test mode to measure the friction curve, the rotation velocity was increased up to 60 rpm by 1 rpm per second as shown in Fig. 10(c) and then once reaching 60 rpm, the rotation velocity was deceased by 1 rpm per second. This test mode was performed consecutively, and the slopes of the velocity corresponding to the sliding speed of approximately 0.01 m/s were linearized and shown in Fig. 11.

Fig. 11(a) shows that the linearized friction-velocity slope for the
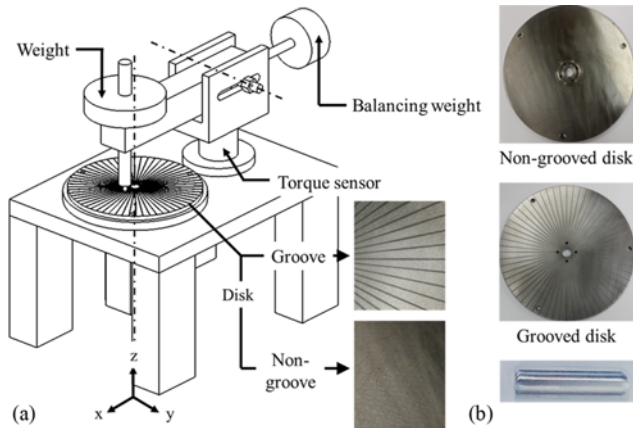
Fig. 9 Schematic diagram of the pin-on-disk: (a) pin-on-disk (b) test specimen
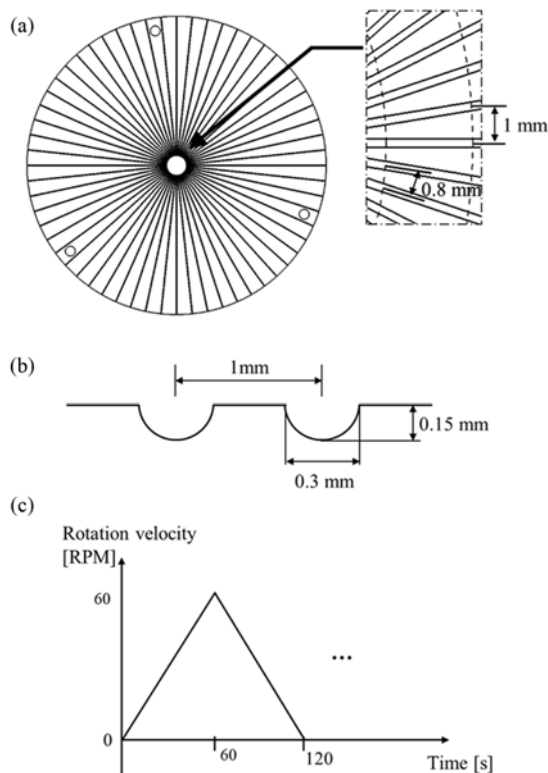
Fig. 10 Pin-on-disk test specimen and test mode: (a) pin-on-disk test specimen (b) dimension of groove surface (c) speed profile

Fig. 11 Linearized friction-velocity slope at 0.01m/s: (a) non-groove surface (b) groove surface

non-groove surface is overall negative. Meanwhile, Fig. 11(b) shows the negative friction-velocity slope of the groove surface for the most of the cycles. A negative friction curve slope increases system instability according to the linear stability theory.[17,18] Thus, the non-groove surface with a negative friction-velocity slope has the higher tendency in the generation of friction noise in terms of the negative friction-velocity slope mechanism.

2.4 Surface topography

Fig. 12 shows the variation of the ball and plate surface topographies, noise onset times, and friction coefficients according to time for the non-groove surface. C and D refer to the behavior of the wear particles which change during friction contact between the ball and plate with time. Noise and vibration did not occur for the range shown in Fig. 12(a) and it can be observed that the friction coefficient was less than 0.3. Here, the beginning of the adhesive phenomenon of the black wear particles on the plate surface can be observed. As time passed, adhesive phenomenon could also be observed at the edges of the plate and the friction coefficient magnitude was increasing. In the range shown in Fig. 12(b), the adhesive phenomenon of the wear particles was more distinctly observable, frictional vibration was generated sporadically, and the average magnitude of the friction coefficient increased to 0.4. For the ranges shown in Figs. 12(c) and (d), friction continued throughout, resulting in the gradual increase of the frictional vibration and friction coefficient. Here, the wide distribution of the wear particles on the ball surface caused by friction can be observed, and the adhesive wear which is the wear particles of the ball adhering to the mild material plate can also be observed in D.[19]

Fig. 13 shows the variation of the ball and plate surface topographies, noise onset times, and friction coefficients according to time for the groove surface. E and F refer to the behavior of the wear particles which change during the friction contact between the ball and plate with time. Frictional vibration did not occur for the range shown in Fig. 13(a) and the average value of the friction coefficient was 0.2. As can be observed in Figs. 13(b)-(d), the friction coefficient increase with the passing of time was relatively insignificant as was the generated vibration levels. In Fig. 13(b), it was observed that the wear particle piled up within the grooves before the initiation of the wear particle adhesive phenomenon on the groove plate surface compared to that of Fig. 13(a). Up to 700 sec, frictional vibration was rarely generated where the pile-up in the groove occurred as shown in Figs. 13(c)-(d). Here, the amount of the wear particles within the grooves
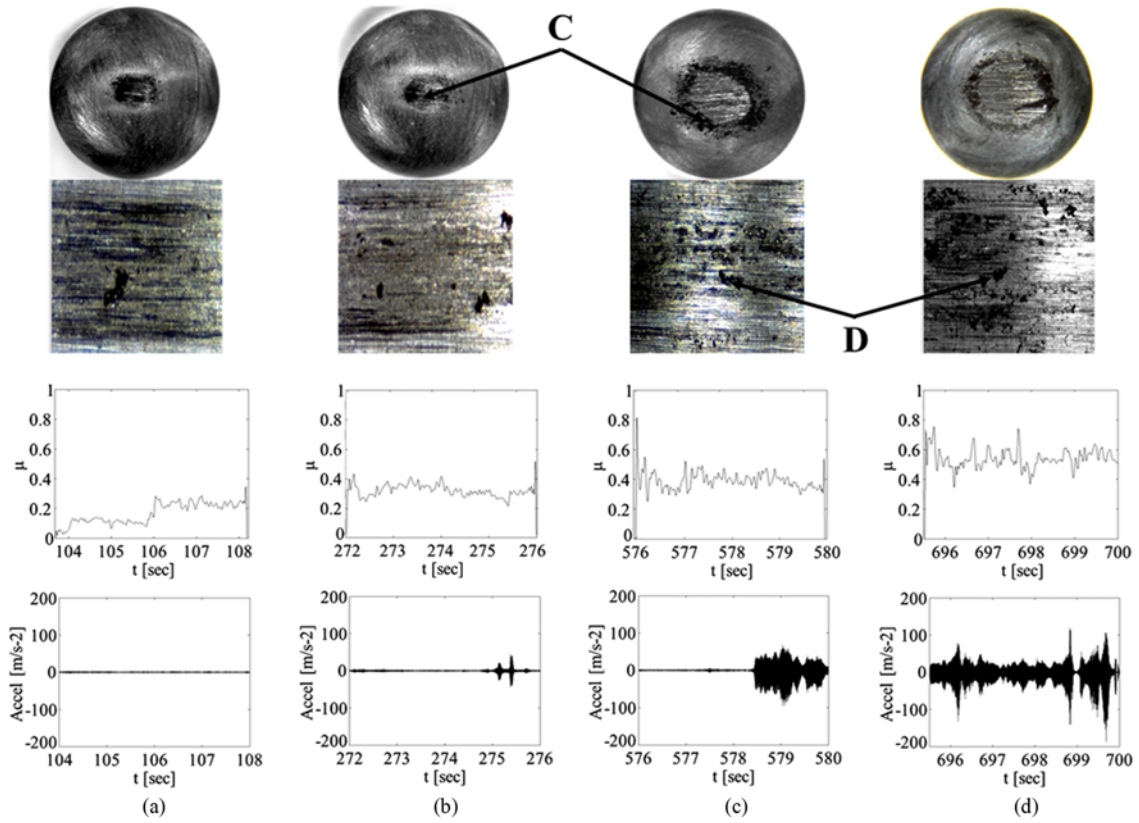
Fig. 12 Contact surface of the non-groove textured surface: (a) from 107 sec to 112 sec (b) from 272 sec to 276 sec (c) from 576 sec to 581 sec (d) from 695 sec to 700 sec
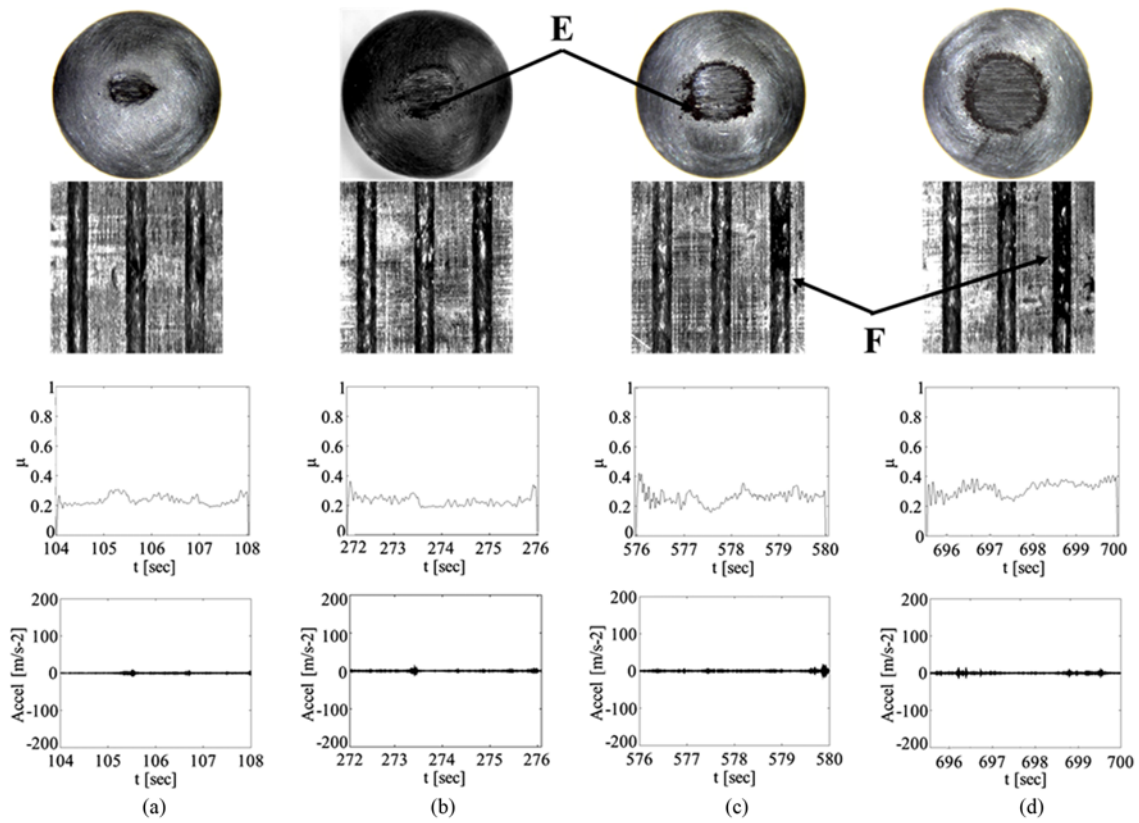
Fig. 13 Contact surface of the groove textured surface: (a) from 107 sec to 112 sec (b) from 272 sec to 276 sec (c) from 576 sec to 581 sec (d) from 695 sec to 700 sec

was larger than that observed in Figs. 13(a) and (b). For the range of Fig. 13(d), the pile-up of the wear particles throughout the groove can be clearly observed and the adhesive phenomenon appeared to be insignificant for the flat area.

Due to the grooves, the wear particles piled up within the groove with time before adhesion occurred on the contact surface. Formations of adhesive wear were less pronounced.

Overall, formations of adhesive wear were frequently observed for the non-groove surface while such signs of adhesive wear were relatively less observable for the groove surface, revealing different wear processes for the two surfaces.[20]

In terms of friction noise, adhesive wear is characterized by the increases in friction coefficient up to a specific time due to the wear particles and vibration magnitude increase. This increase in friction coefficient can cause friction noise due to mode coupling instability. The groove surface, which showed relatively less adhesive wear and with longer time, had a lower propensity for mode coupling instability as the wear particles fall within the grooves from the contact surface before adhesion occurs, resulting in a relatively low friction coefficient until a specific time.[21]

3. Conclusions

In this study, the mechanism of friction noise produced on the contact surface between the ball and groove made on a plate was experimentally analyzed. Also, the wear conditions were observed according to time to analyze the wear phenomenon through the wear particle behavior on the non-groove textured and groove textured surfaces. The non-groove textured surface condition facilitated mode coupling and negative friction-velocity slope instability over the groove textured surface, and it was predicted that this result would make it easier for friction noise to occur. Moreover, the tribo-surface analysis result revealed different wear processes. The following conclusions were obtained.

1) In the experimental results, friction noise occurred at about 5 kHz for the different surface conditions of non-groove textured and groove textured surfaces. The onset time (near 300 sec) of the friction noise for the non-groove textured surface was much faster than that of the groove textured surface and the value of the vibration level was also maximum 4 dB greater.

2) The friction coefficient according to time was maximum 0.3 higher for the non-groove textured surface, and the negative friction-velocity slope was mainly observed for the non-groove textured surface. The non-groove textured surface was favorable for the onset of instability due to the mode coupling and negative friction-velocity slope which are friction noise mechanisms.

3) Wear particles are produced from the worn surface due to ploughing and cutting. Here, adhesive wear is observed for the non-groove texture surface and the friction coefficient rapidly increases due to surface debris. However, for the groove texture surface, surface debris falls within the grooves before the initiation of adhesive wear, resulting in a relatively slow increase in the friction coefficient. In addition, the noise onset time was much faster for the non-groove textured surface with adhesive wear occurring overall compared to the groove textured surface with less observable adhesive wear.

ACKNOWLEDGEMENT

REFERENCES

1. Chen, G. X., Zhou, Z. R., Kapsa, P., and Vincent, L., "Effect of Surface Topography on Formation of Squeal Under Reciprocating Sliding," Wear, Vol. 253, No. 3, pp. 411-423, 2002.

2. Chen, G. X., Zhou, Z. R., Kapsa, P., and Vincent, L., "Experimental Investigation into Squeal Under Reciprocating Sliding," Tribology International, Vol. 36, No. 12, pp. 961-971, 2003.

3. Jibiki, T., Shima, M., Akita, H., and Tamura, M., "A Basic Study of Friction Noise Caused by Fretting," Wear, Vol. 251, No. 1, pp. 1492-1503, 2001.

4. Yuan, S., Huang, W., and Wang, X., "Orientation Effects of Micro-Grooves on Sliding Surfaces," Tribology International, Vol. 44, No. 9, pp. 1047-1054, 2011.

5. Mo, J. L., Wang, Z. G., Chen, G. X., Shao, T. M., Zhu, M. H., and Zhou, Z. R., "The Effect of Groove-Textured Surface on Friction and Wear and Friction-Induced Vibration and Noise," Wear, Vol. 301, Nos. 1-2, pp. 671-681, 2013.

6. Saeidi, F., Meylan, B., Hoffmann, P., and Wasmer, K., "Effect of Surface Texturing on Cast Iron Reciprocating Against Steel Under Starved Lubrication Conditions: A Parametric Study," Wear, Vol. 348, pp. 17-26, 2016.

7. Zhang, H., Hua, M., Dong, G.-n., Zhang, D.-y., and Chin, K.-S., "A Mixed Lubrication Model for Studying Tribological Behaviors of Surface Texturing," Tribology International, Vol. 93, Part B, pp. 583-592, 2016.

8. Wang, D. W., Mo, J. L., Wang, Z. G., Chen, G. X., Ouyang, H., and Zhou, Z. R., "Numerical Study of Friction-Induced Vibration and Noise on Groove-Textured Surface," Tribology International, Vol. 64, pp. 1-7, 2013.

9. Wang, D. W., Mo, J. L., Ouyang, H., Chen, G. X., Zhu, M. H., and Zhou, Z. R., "Experimental and Numerical Studies of Friction-Induced Vibration and Noise and the Effects of Groove-Textured Surfaces," Mechanical Systems and Signal Processing, Vol. 46, No. 2, pp. 191-208, 2014.

10. He, B., Chen, W., and Jane Wang, Q., "Surface Texture Effect on Friction of a Microtextured Poly (Dimethylsiloxane)(PDMS)," Tribology Letters, Vol. 31, No. 3, pp. 187-197, 2008.

11. Wang, X., Liu, W., Zhou, F., and Zhu, D., "Preliminary Investigation of the Effect of Dimple Size on Friction in Line Contacts,"

Tribology International, Vol. 42, No. 7, pp. 1118-1123, 2009.

12. Bergman, F., Eriksson, M., and Jacobson, S., "Influence of Disc Topography on Generation of Brake Squeal," Wear, Vols. 225-229, Part 1, pp. 621-628, 1999.

13. Sherif, H., "Investigation on Effect of Surface Topography of Pad/ Disc Assembly on Squeal Generation," Wear, Vol. 257, No. 7, pp. 687-695, 2004.

14. Kang, J., "Squeal Analysis of Gyroscopic Disc Brake System Based on Finite Element Method," International Journal of Mechanical Sciences, Vol. 51, No. 4, pp. 284-294, 2009.

15. Kang, J., Krousgrill, C. M., and Sadeghi, F., "Analytical Formulation of Mode-Coupling Instability in Disc-Pad Coupled System," International Journal of Mechanical Sciences, Vol. 51, No. 1, pp. 52-63, 2009.

16. Kang, J., Krousgrill, C. M., and Sadeghi, F., "Dynamic Instability of a Thin Circular Plate with Friction Interface and Its Application to Disc Brake Squeal," Journal of Sound and Vibration, Vol. 316, No. 1, pp. 164-179, 2008.

17. Kang, J., Krousgrill, C. M., and Sadeghi, F., "Comprehensive Stability Analysis of Disc Brake Vibrations Including Gyroscopic, Negative Friction Slope and Mode-Coupling Mechanisms," Journal of Sound and Vibration, Vol. 324, No. 1, pp. 387-407, 2009.

18. Ouyang, H., Mottershead, J. E., Cartmell, M. P., and Friswell, M. I., "Friction-Induced Parametric Resonances in Discs: Effect of a Negative Friction-Velocity Relationship," Journal of Sound and Vibration, Vol. 209, No. 2, pp. 251-264, 1998.

19. Straffelini, G., "A Simplified Approach to the Adhesive Theory of Friction," Wear, Vol. 249, Nos. 1-2, pp. 78-84, 2001.

20. Stachowiak, G. P., Stachowiak, G. W., and Podsiadlo, P., "Automated Classification of Wear Particles Based on their Surface Texture and Shape Features," Tribology International, Vol. 41, No. 1, pp. 34-43, 2008.

21. Rusli, M. and Okuma, M., "Effect of Surface Topography on Mode-Coupling Model of Dry Contact Sliding Systems," Journal of Sound and Vibration, Vol. 308, No. 3, pp. 721-734, 2007.